Electrochemistry Communications 111 (2020) 106647

Contents lists available at ScienceDirect

Electrochemistry Communications

journal homepage: www.elsevier.com/locate/elecom

Active and stable graphene supporting trimetallic alloy-based electrocatalyst for hydrogen evolution by seawater splitting

Maria Sarno[a,b,*], Eleonora Ponticorvo[b], Davide Scarpa[c]

[a] Department of Physics "E.R. Caianiello", University of Salerno, Via Giovanni Paolo II, 132, 84084 Fisciano, SA, Italy
[b] NANO_MATES, Research Centre for Nanomaterials and Nanotechnology at the University of Salerno, University of Salerno, Via Giovanni Paolo II, 132, 84084 Fisciano, SA, Italy
[c] Department of Industrial Engineering, University of Salerno, Via Giovanni Paolo II, 132, 84084 Fisciano, SA, Italy

ARTICLE INFO

Keywords:
Trimetallic alloy
NiRuIr alloy
Seawater
Hydrogen evolution reaction
High stability
High H_2 production

ABSTRACT

The hydrogen evolution reaction (HER), adopting seawater as an electrolyte solution, is a promising and more sustainable alternative for the production of hydrogen, yet requiring more economic, highly efficient and stable electrocatalysts than the current ones. Herein, the synthesis of a Ni, Ru, Ir-based and graphene-supported nanostructured catalyst through an easily scalable, cost-effective, surfactant-free approach has been proposed. XRD, SEM, TEM images and EDX maps showed the formation of trimetallic NiRuIr alloy nanoparticles (average diameter: 8 nm) supported on a few-layer graphene. After characterization, the HER stability and activity of the sample were tested in a 0.5 M H_2SO_4, in a KCl neutral solution as well as in real seawater. In the acidic electrolyte environment a 0.06 V overpotential was maintained even after 11,000 cycles and the Tafel slope recorded was very low (28 mV/dec). In the neutral solution a very low overpotential (0.10 V) and a low Tafel slope (72 mV/dec) were also obtained. Furthermore, in real seawater the sample exhibits a Tafel slope of 48 mV/dec, maintains a low overpotential of 0.08 V for 250 cycles and a constant current density for 200 h of test without significant losses and with almost a 100% hydrogen production efficiency. The results obtained proved the remarkable HER performance of the synthesized electrocatalyst, especially in real seawater in virtue of synergistic alloying effects and the presence of the graphene support.

1. Introduction

Nowadays, water electrolysis as a promising technique for the production of highly pure hydrogen is on the rise. The search for new cost-effective electrocatalysts capable of ensuring high activity towards the hydrogen evolution reaction (HER) and good stability in the electrolysis environment is the most crucial step for the industrial-scale development of this technology [1]. To date, most of the current literature focuses on the HER characterization in a mixture of distilled water and acid or alkaline electrolytes. On the other hand, an interesting and attractive alternative would be the electrochemical generation of H_2 from seawater. Indeed, about 97% of the water present in nature originates from seas and oceans; hence, it is easily, abundantly and freely available as seawater [2]. In addition, by directly feeding seawater to an electrolyzer, the expensive and complex purification and desalinization processes are not required. Rather, seawater salts are crucial, acting as charge carriers during electrolysis. As a consequence, since these carriers are highly present in seawater, further addition of acid or basic electrolytes cannot be needed. Therefore, production costs are reduced, i.e. no cost for water distillation and reduced costs for disposal. On the other hand, the high presence and variety of salts can generate a corrosive environment for the catalysts. Moreover, in the unpurified seawater, there are hundreds of different impurities, which might lead to catalyst poisoning.

However, to date, there are few studies dealing with the production of hydrogen from seawater, with results which are still far from being satisfactory, especially with respect to the use of a catalyst consisting predominantly of inexpensive materials. In order to meet these challenges, is fundamental the design of new, economical and efficient nanostructured catalysts for HER catalysis in seawater, capable of ensuring low energy supply, high tolerance towards impurities and high stability and resistance in a corrosive environment. In particular, the main effort must be done in order to improve activity and stability in seawater. In this scenario, the use of a trimetallic alloy enables wider leeway in the choice of components and exploitation of new alloy properties and functionality, to optimize activities, costs and resistance

* Corresponding author at: Department of Physics "E.R. Caianiello", University of Salerno, Via Giovanni Paolo II, 132, 84084 Fisciano, SA, Italy.
E-mail address: msarno@unisa.it (M. Sarno).

https://doi.org/10.1016/j.elecom.2019.106647
Received 20 November 2019; Received in revised form 18 December 2019; Accepted 19 December 2019
Available online 23 January 2020

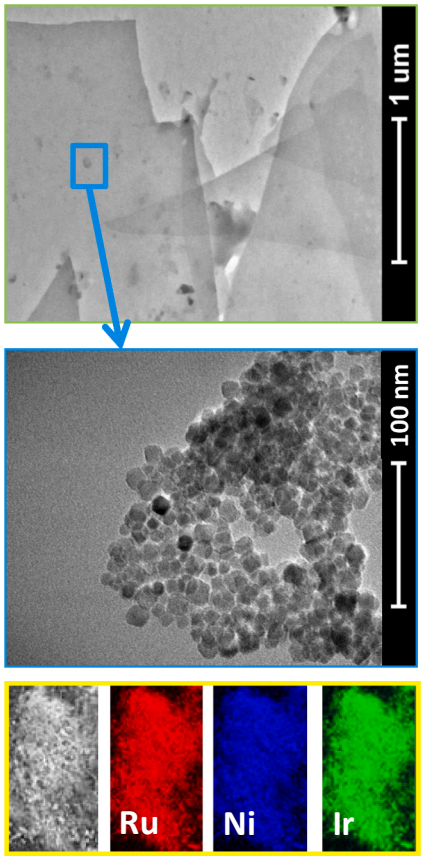

Fig. 1. TEM images of NiRuIr_G nanocomposite and EDX maps of ruthenium, nickel and iridium.

to corrosion. Pure platinum has been accurately explored in virtue of its remarkably high electrocatalytic activity towards a large number of reactions. Nonetheless, the industrial-scale adoption of Pt has been significantly hindered by its scarce availability, high cost and low tolerance to poisoning, leading to the need for better alternatives to it [3]. Iridium is a Pt-group metal which shows the highest corrosion resistance among metals, high stability towards dissolution and oxidation, as well as a good activity towards HER with a wide range of oxidation states [4]. On the other hand, it is among the platinum-group metals yet less expensive than Pt, ruthenium has attracted increasing interest for the HER catalysis in alkaline media since it efficiently favors H_2O dissociation [5]. Nickel is the commercial catalyst for HER and considered a good catalyst for HER in alkaline solutions owing to its high activity and low cost [6]. Furthermore, it has been proved that the presence of carbonaceous materials as support can help stabilize metals by favoring water dissociation on it, hence increasing their HER activity

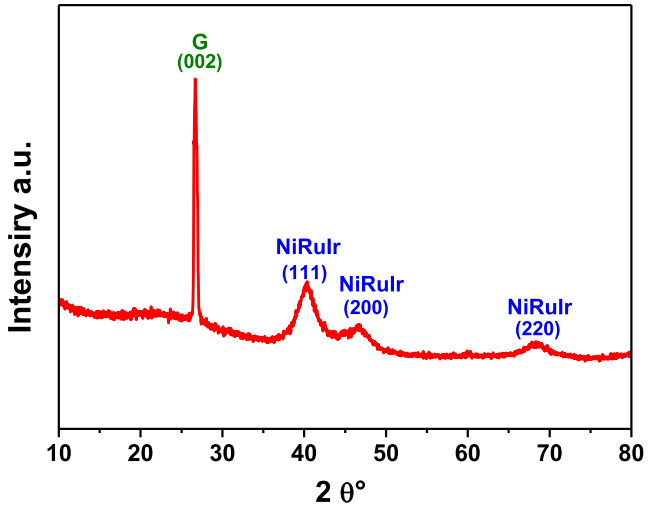

Fig. 3. XRD spectrum of NiRuIr_G nanocomposite.

[7]. Among carbon materials, graphene is very promising [8] as effective catalyst support in virtue of its high stability and electron mobility as well as of its high tolerance towards impurities.

Herein, the preparation of a novel NiRuIr_G nano-structured catalyst for hydrogen generation from seawater splitting was reported. The nanocatalyst consists of a Ni/Ru/Ir nanoalloy laying on few-layer graphene. The catalyst synthesis was designed and obtained by means of a surfactant-free approach in ethylene glycol. Afterward, the synthesized sample was tested towards HER in acid and neutral water, and in real seawater solutions exhibiting very promising performances, in particular low overpotentials and Tafel slopes as well as higher current densities.

2. Materials and methods

2.1. NiRuIr_G nanohybrid preparation

For the synthesis, a surfactant-free approach was chosen [9] and designed here for the specific new nanocatalyst. For NiRuIr_G catalyst: ruthenium(III) chloride hydrate (0.5 mmol), nickel(II) chloride (0.5 mmol) and sodium hydroxide (0.288 g) were added to a solution of ethylene glycol (66 mL) and water (6 mL); the mixture was stirred for 30 min at 25 °C and then heated up till 130 °C for an hour; 3 mL of solution was withdrawn from the system; iridium(III) chloride (0.5 mmol) was added to the withdrawn solution, which was then re-injected into the reactor and maintained at 130 °C for 2 additional hours under nitrogen flow. Afterward, the solution was cooled down to room temperature, few-layer graphene (0.5 g) was added and the mixture was further stirred for 24 h without increasing its temperature. Finally, it was treated with acetone in order to remove ethylene glycol.

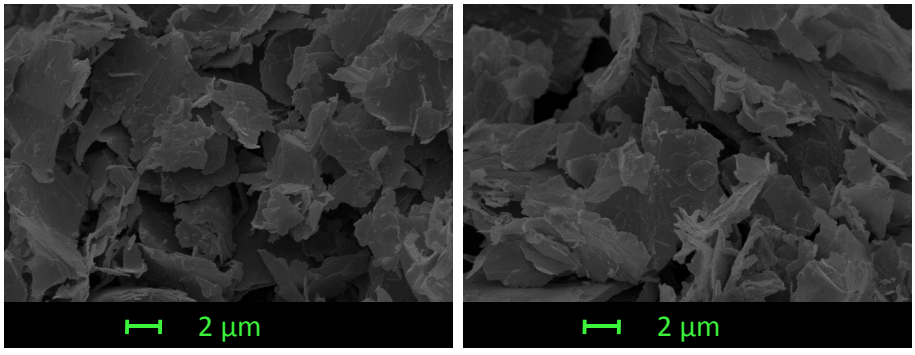

Fig. 2. SEM images of NiRuIr_G nanocomposite.

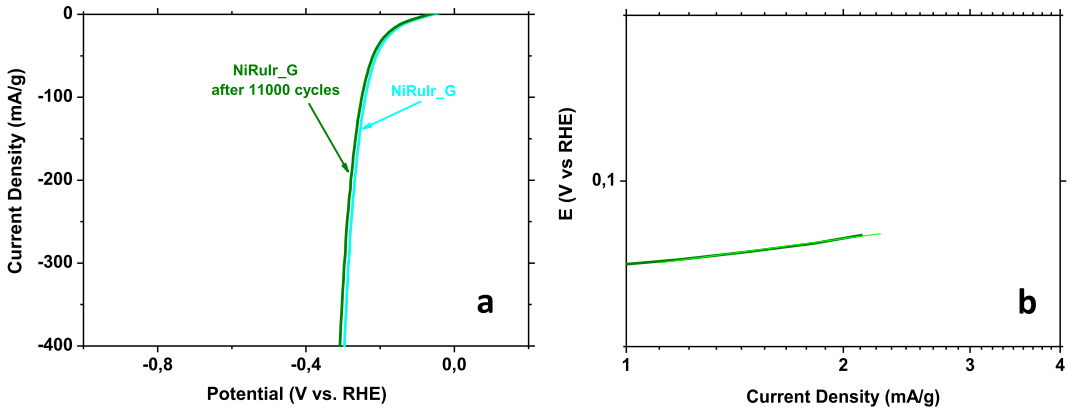

Fig. 4. (a) Polarization curves before and after 11,000 cycles and (b) Tafel plot for NiRuIr_G nanohybrid recorded at 20 mV/s in a 0.5 M H_2SO_4 electrolyte.

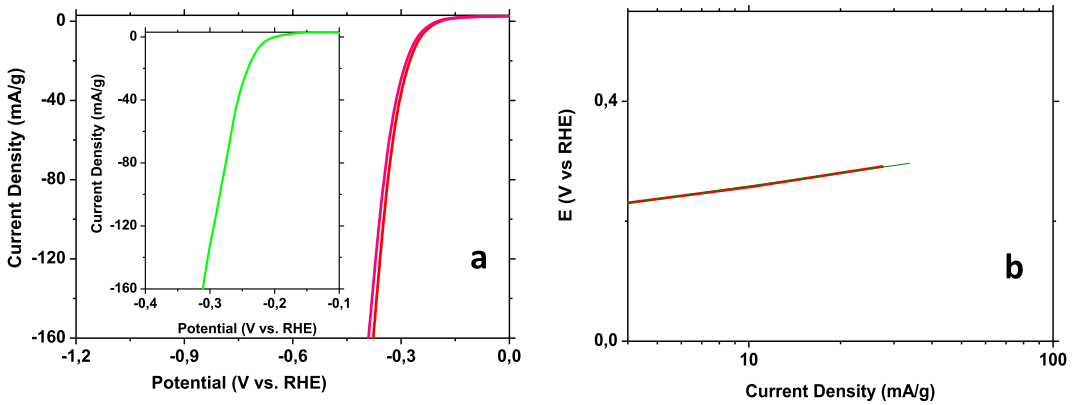

Fig. 5. (a) Polarization curve before and after 11,000 cycles recorded at 20 mV/s in a KCl aqueous electrolyte, in the inset polarization curve recorded at 20 mV/s in a KOH aqueous electrolyte. (b) Tafel plot of NiRuIr_G nanohybrid recorded at 20 mV/s in a KCl aqueous electrolyte.

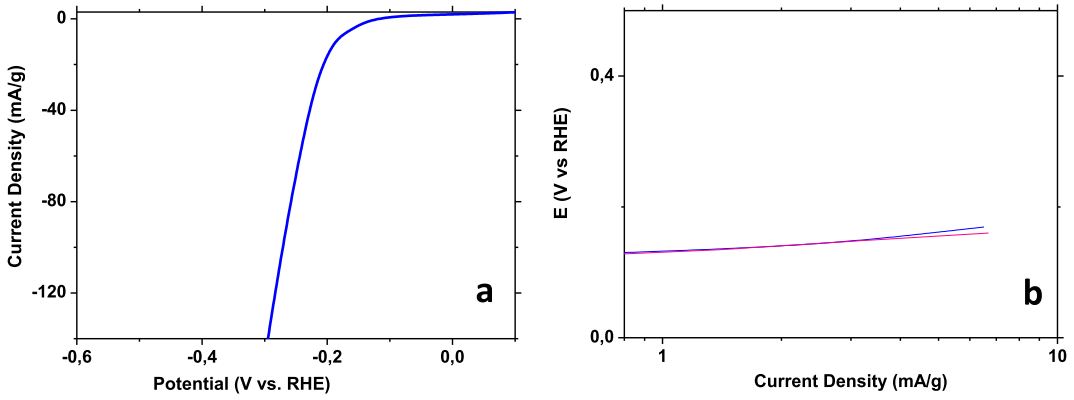

Fig. 6. (a) Polarization curve and (b) Tafel plot of NiRuIr_G nanohybrid recorded at 20 mV/s in real seawater.

Finally, the sample underwent a post-synthesis treatment in an autoclave under the following conditions: the reaction proceeded for 3 h at 205 °C and at 10 bar under a 5 vol% hydrogen/nitrogen flow (5 vol% H_2).

2.2. Characterization

A FEI Tecnai electron microscope was used to obtain transmission electron microscopy (TEM) images, whereas field emission scanning electron microscopy (FESEM) images were acquired through a LEO 1525 electron microscope, equipped with an energy dispersive X-ray (EDX) probe. Moreover, a Bruker D8 X-ray diffractometer (CuKα) was used for XRD measurements.

To perform electrochemical tests, an ink with the sample was dropped onto a DRP-110 Screen Printed Electrode. Electrochemical tests were carried out through an Autolab PGSTAT302N potentiostat. Lastly, the output gas was examined through a gas chromatography-mass spectrometry analysis, through a Thermo Scientific FOCUS GC-ISQ Single Quadrupole MS and the H_2 production efficiency was calculated [10].

3. Results and discussion

3.1. Morphological characterization

TEM images in Fig. 1 show the existence of nanoparticles with a uniform size anchored on few-layer graphene. The nanoparticles have an average diameter of 8 nm with a standard deviation of 1.8 nm.

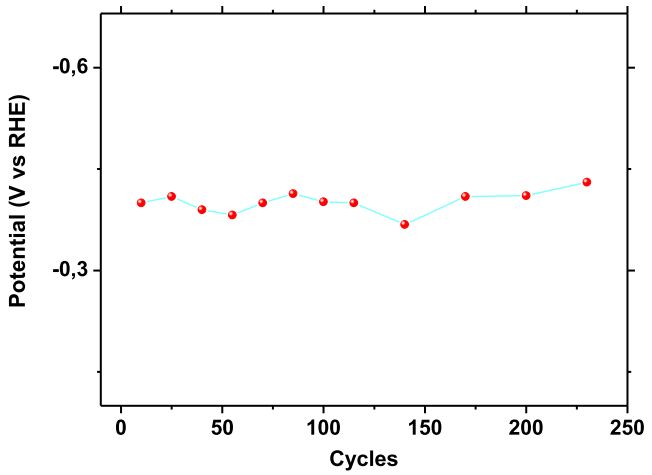

Fig. 7. Potential of NiRuIr_G nanohybrid in real seawater as a function of different cycles.

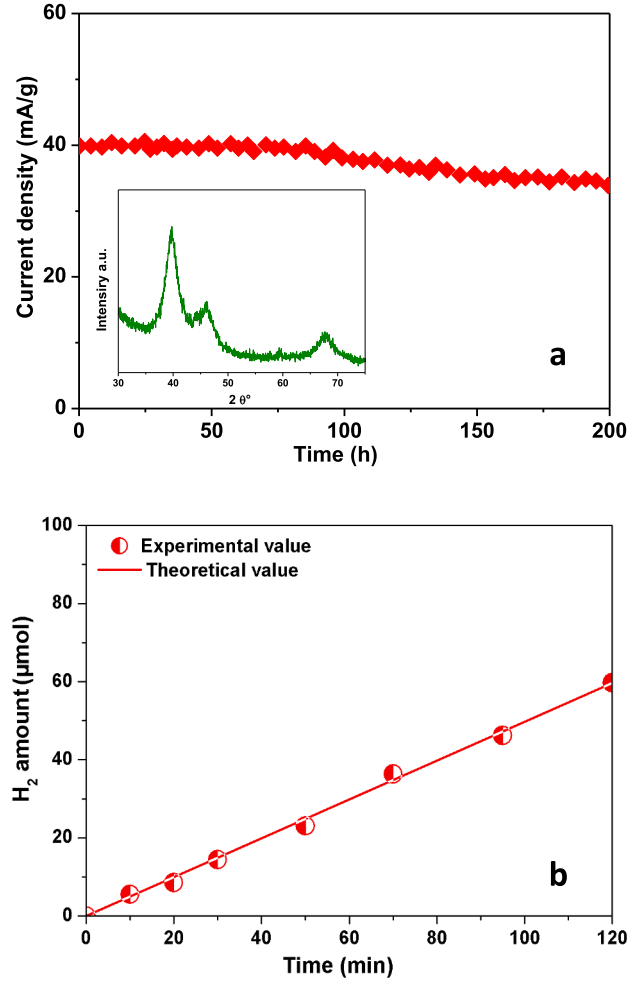

Fig. 8. Current-Time curve in real seawater, in the inset the NiRuIr_G nanohybrid XRD profile after 200 h of electrolysis (a), hydrogen production efficiency for HER under potentiostatic electrolysis (b).

Energy dispersive spectroscopy (EDS) was also carried out, showing an Ir/Ru/Ni atomic ratio of 3.2:3.0:3.1, which is in good agreement with the percentages of metal precursors adopted for the synthesis. Furthermore, the EDX maps of the metals are reported. The maps of Ir, Ru and Ni are superimposable, which suggests a homogeneous distribution of the three metals in the nanostructure and, therefore, the trimetallic alloy nature of the sample. In addition, SEM images of the synthesized sample are reported in Fig. 2, showing the existence of a three-dimensional network of graphene flakes strictly connected to each other.

3.2. X-ray diffraction analysis

Fig. 3 shows that the diffraction peaks in the Ir-Ru-Ni nanoparticles matches the (1 1 1), (2 0 0) and (2 2 0) typical planes of the iridium fcc structure, shifted to slightly higher 2θ values. The absence of peaks related to the hcp structure of pure ruthenium and of the fcc structure of pure nickel, as well as the aforementioned angle shift, likely due to a modification of the lattice constant caused by the incorporation of Ru and Ni atoms, suggests the existence of a trimetallic alloy [11]. Moreover, in the same pattern, the diffraction peak related to the (0 0 2) reflection of few-layer graphene can be detected at $2\theta = 26.0^{\circ}$, suggesting the existence of a highly ordered crystal structure with an interlayer distance equals to 3.4 Å, more details regarding the nanosheets distribution has been previously reported [12,13].

3.3. Electrochemical hydrogen evolution reaction

Firstly, the HER activity of NiRuIr_G was tested in a 0.5 M H_2SO_4 solution at 1 and 11,000 cycles of the test (Fig. 4a). As can be seen from the polarization curves at 20 mV/s, the sample exhibits a low overpotential whose value remains approximately the same one (0.06 V), even after 11,000 cycles of test, hence suggesting the high stability of the synthesized material in acidic media. In Fig. 4b, the corresponding Tafel plot is reported and a very low Tafel slope of 28 mV/dec was recorded, suggesting that the reaction proceeds through the Volmer-Tafel mechanism [14]. In order to minimize the harmful environmental impacts, the electro-catalytic behavior towards HER of NiRuIr_G in a neutral KCl aqueous solution was also tested. The polarization curve, even after 11,000 cycles of test, and the corresponding Tafel plot in Fig. 5a and b show an overpotential of 0.10 V, almost comparable with the one obtained with an H_2SO_4-based electrolyte, a Tafel slope of 72 mV/dec, which suggests that the electrochemical hydrogen production proceeds quickly also in this case and remarkable stability. HER onset potential in alkaline solutions, higher than that obtained in acidic media, was also evaluated (Fig. 5a, inset). However, since a neutral solution of a single salt cannot be found in a real environment, the HER behavior of the synthesized sample was tested adopting a real seawater solution as the electrolyte, too. Fig. 6a and b show the polarization curve and the corresponding Tafel plot, evidencing that increased performance was obtained in real seawater likely due to the higher amount of dispersed electrolytes.

Fig. 7 shows that NiRuIr_G roughly remains at an identical overpotential level at different sweep voltammetry cycles from the first one till the 250th one, which indicates the high stability of the sample in real seawater as well. The sample stability in the real seawater electrolyte is confirmed also by the chronoamperometric measurement reported in Fig. 8a. The inset of the same figure shows the X-ray diffraction profile of the catalyst after 200 h of usage. A small shift of the relevant peaks was observed as a results of an Ir enrichment in the alloy. At a constant potential of 0.23 V, the corresponding current density of 40 mA/g was recorded and only a 10% current loss was recorded within 200 h. In Fig. 8b the hydrogen production efficiency for HER under potentiostatic electrolysis promoted by NiRuIr_G, is shown, highlighting the effectiveness of the catalyst. In particular, the amount of hydrogen produced using the nanohybrid in the real seawater solution was evaluated. The micromoles of hydrogen produced at several times were detected through gas chromatography-mass spectrometry and reported in Fig. 8b (dots). The experimental data are in good agreement with the theoretical ones obtained when considering the amount of charges passing through the system (straight line in the same Figure), which proves a remarkable H_2 production efficiency.

Table 1
Comparison of the HER performance in real seawater between NiRuIr_G nanohybrid and the most performing electrocatalysts reported in literature.

Catalyst	Tafel slope [mV/dec]	Overpotential [V]	Stability	Ref.
Ni-Mo(1)_11Mo/Nif	105	~0.152 (vs Ag/AgCl)	–	[15]
Co,N-codoped CNT	~159 (buffer solution ph7)	~0.5 (vs RHE)	No significant current losses within 10 h	[7]
CoMoP@C	~140 (buffer solution ph7)	~0.3 (vs RHE)	No significant current losses within 10 h	[16]
RuCo/Ti	107	0.253(vs RHE)	30% of current loss over 12 h	[17]
RuCoMo/Ti	140	0.354(vs RHE)	No significant current losses within 12 h	[17]
Ni-Fe-C	–	~0.76(vs Hg/HgO)	–	[18]
MoS_2 QD areogel	–	~0.25 (vs RHE)	At 80 mA/g, potential level is constant for 150 cycles	[19]
Commercial Pt	–	Negligible (vs RHE)	At 80 mA/g, potential increases from 0.6 V to over 0.8 V within 150 cycles	[19]
Pt NPs	45.8	~0.23(vs RHE)	~8% of current loss over 13.9 h	[20]
PtRuMo/Ti	44	~0.1(vs RHE)	~15% of current loss over 172 h	[20]
NiRuIr_G	48	~0.08(vs RHE)	Potential level is constant for 250 cycles; ~10% of current loss over 200 h	This work

For comparison, the HER activity parameters and the stability behavior of the most performing electrocatalysts in real seawater are reported in Table 1 [7,15–20]. Pt performance are not remarkable in this type of electrolytic environment. Indeed, although being a benchmark catalyst in acid electrolytes, it can be easily poisoned due to the high presence of seawater impurities. The excellent performance of our nanocatalyst can be ascribed to intrinsic characteristics of the components and due to synergistic alloying effects and, finally, to the graphene support. In particular, the main reasons of the improved performance are:

1. the choice of the highly active Ir, and the Ir and Ru stability.
2. the different work functions between the metals, inducing an electron-enriched Ir surface, i.e. high activity [20], strong interaction with H^+ ions and increased stability [21], repulsion of Cl^- ions due the highly negatively charged Ir surface.
3. increased anti-corrosion properties, which can be ascribed to competitive dissolution reactions [20] between the different components into the alloy with Cl_2 dispersed in seawater. In particular, dissolution of the three metals in the presence of Cl^- is spontaneous (ΔG strongly negative), but for Ir the ΔG absolute value is much smaller.
4. nanoparticles stability induced by the highly conductive graphene carpet, decreasing charge-transfer resistance at the catalyst/electrolyte interface and increasing electrochemical conductivity. It can be also imagined a role of graphene in helping catalysis thanks to H^+ adsorption, and protecting catalyst from poisoning [16].

4. Conclusions

In summary, the synthesis of a Ni, Ru, Ir-based and graphene-supported nano-structured catalyst was successfully carried out through a surfactant-free method. Analyses of SEM and TEM images, EDX maps and XRD spectrum showed the formation of trimetallic NiRuIr alloy nanoparticles supported on a few-layer graphene. Afterward, the sample HER activity and stability were tested in a 0.5 M H_2SO_4, in a KCl neutral solution as well as in real seawater, exhibiting excellent performance, which can be due to many reasons. Firstly, iridium, which is at the top of the Trasatti's volcano plot, guarantees a high activity towards hydrogen evolution and gives the major contribution to the stability of the alloy both in acid and seawater environment. Secondly, the difference in work functions between the metals in the alloy promotes the accumulation of electrons on the Ir surface, hence further increasing the activity. Moreover, the negative charges accumulated on Ir can prevent Cl^- anions attack, too. Moreover, the dissolution reaction with the gaseous Cl_2 is the least spontaneous on Ir compared to the other alloy species, which further increases the sample stability. Eventually, the highly conductive graphene network stabilizes the nanoparticles anchored on it, reduces the charge-transfer resistance at the catalyst/electrolyte interface, increases the electrochemical conductivity and offers further active sites for the H^+ ions adsorption and catalyst preservation.

CRediT authorship contribution statement

Maria Sarno: Supervision. **Eleonora Ponticorvo:** Methodology, Investigation. **Davide Scarpa:** Investigation, Data curation.

Declaration of Competing Interest

The authors declare that they have no known competing financial interests or personal relationships that could have appeared to influence the work reported in this paper.

Appendix A. Supplementary data

Supplementary data to this article can be found online at https://doi.org/10.1016/j.elecom.2019.106647.

References

[1] M. Sarno, C. Cirillo, E. Ponticorvo, P. Ciambelli, Chem. Eng. Trans. 43 (2015) 943–948, https://doi.org/10.3303/CET1543158.
[2] S.A. Kalogirou, Prog. Energy Combust. Sci. 31 (2005) 242–281.
[3] D. Liu, L. Li, T. You, J. Colloid Interface Sci. 487 (2017) 330–335.
[4] S. Štrbac, I. Srejić, Z. Rakočević, J. Electrochem. Soc. 165 (2018) J3335–J3341.
[5] C.H. Chen, D. Wu, Z. Li, R. Zhang, C.G. Kuai, X.R. Zha, C.K. Dong, S.Z. Qiao, H. Liu, X.W. Du, Adv. Energy Mater. 9 (2019) 1803913.
[6] X.X. Yu, T.Y. Hua, X. Liu, Z.P. Yan, P. Xu, P.W. Du, A.C.S. Appl, Mater. Interfaces 6 (2014) 15395–15402.
[7] S. Gao, G.D. Li, Y. Liu, H. Chen, L.L. Feng, Y. Wang, M. Yang, D. Wang, S. Wang, X. Zou, Nanoscale 7 (2015) 2306–2316.
[8] M. Sarno, D. Sannino, C. Leone, P. Ciambelli, J. Mol. Catal. A-Chem. 357 (2012) 26–38.
[9] M. Sarno, E. Ponticorvo, D. Scarpa, Nanotechnology 30 (2019) 394004.
[10] M. Sarno, E. Ponticorvo, D. Scarpa, Chem. Eng. J. 377 (2019) 120600.
[11] K.W. Park, J.H. Choi, B.K. Kwon, S.A. Lee, Y.E. Sung, H.Y. Ha, S.A. Hong, H. Kim, A. Wieckowski, J. Phys. Chem. B 106 (2002) 1869–1877.
[12] C. Lee, X. Wei, J.W. Kysar, J. Hone, Science 321 (2008) 385–388.
[13] L. Guadagno, M. Sarno, U. Vietri, M. Raimondo, C. Cirillo, P. Ciambelli, RSC Adv. 5 (2015) 27874–27886.
[14] Y. Li, H. Wang, L. Xie, Y. Liang, G. Hong, H. Dai, J. Am. Chem. Soc. 133 (2011) 7296–7299.
[15] F. Golgovici, A. Pumnea, A. Petica, A.C. Manea, O. Brincoveanu, M. Enachescu, L. Anicai, Chem. Pap. 72 (2018) 1889–1903.
[16] Y.Y. Ma, C.X. Wu, X.J. Feng, H.Q. Tan, L.K. Yan, Y. Liu, Z.H. Kang, E.B. Wang, Y.G. Li, Energy Environ. Sci. 10 (2017) 788–798, https://doi.org/10.1039/C6EE03768B.
[17] X. Niu, Q. Tang, B. He, P. Yang, Electrochim. Acta 208 (2016) 180–187.
[18] L.J. Song, H.M. Meng, Int. J. Hydrog. Energy 35 (2010) 10060–10066.
[19] I.W.P. Chen, C.H. Hsiao, J.Y. Huang, Y.H. Peng, C.Y. Chang, A.C.S. Appl, Mater. Interfaces 11 (2019) 14159–14165.
[20] H. Li, Q. Tang, B. He, P. Yang, J. Mater. Chem. A 4 (2016) 6513–6520.
[21] Y. Kuang, M.J. Kenney, Y. Meng, W.H. Hung, Y. Liu, J.E. Huang, R. Prasanna, P. Li, Y. Li, L. Wang, M.C. Lin, M.D. McGehee, X. Sun, H. Dai, Proc. Natl. Acad. Sci. USA 116 (2019) 6624–6629.